

Higher-Order Effects of Electron Capture and Loss to the Continuum in Ion-Atom Collisions

W. Oswald, R. Schramm, and H.-D. Betz

Sektion Physik, Universität München, 8046 Garching, Federal Republic of Germany

(Received 1 August 1988)

We have investigated electron capture and loss into the continuum of projectiles resulting from single ion-atom collisions. It is revealed that characteristic shape parameters of the well-known cusp in the velocity spectrum observed in the forward direction depend markedly on the experimental resolution. This hitherto unobserved behavior can be explained by higher-order effects in the transition amplitudes of the double-differential production cross section.

PACS numbers: 34.70.+e

When ions collide with target atoms electrons can be captured into the continuum of the projectile (ECC) or initially bound projectile electrons can become excited into the projectile continuum (ELC). In both cases, these electrons travel along with almost the same velocity as the ion (v_p) and can therefore be observed only at and near 0° in the forward direction, giving rise to a cusp-shaped peak in the velocity spectrum of electrons. Ever since its first evidence¹ this phenomenon has been studied theoretically²⁻⁷ and experimentally⁸⁻¹¹ and is thought to be essentially understood.

Previous experiments with various ion beams and different gas-target species have resulted in cusp shapes which turned out to be either quite symmetric or very asymmetric depending on whether ELC or ECC was studied. It has always been assumed that, for a given collision system, the (FWHM) width Γ of the cusp depends on the angular resolution Θ_0 , $\Gamma \sim \Theta_0$, while shape and degree of asymmetry are thought to remain unaffected.^{8,11} This expectation has been tested systematically only for $H^+ \rightarrow He$ where it was found to be essentially correct except for the smallest collision velocities used.⁸ As a consequence, many authors have represented the double-differential cross section by a series expansion with Legendre polynomials and extracted the relevant coefficients from an analysis of a cusp shape observed for a single experimental angular resolution. It has to be assumed, of course, that these parameters should be characteristic for the system studied, independent of the geometry of the apparatus employed.^{8,11}

It is the purpose of this Letter to demonstrate that in many collision systems cusps can exhibit a more complicated structure than hitherto believed. Our data are in good agreement with previous results obtained for $\Theta_0 \geq 1^\circ$, but a pronounced and unexpected change of line shape is revealed when Θ_0 is improved. Apparently, a characteristic feature of ECC and ELC processes has gone unnoticed for a long time and theoretical descriptions of the process must be extended in many cases to incorporate the newly observed features of continuum state production.

The Munich tandem-accelerator facility was used to

prepare beams of 25- to 80-MeV oxygen and 110-MeV bromine ions with initial charges ranging from $4+$ to $8+$ and $10+$ to $24+$, respectively. The beams were collimated to a diameter of 0.8 mm and a divergence of less than 0.05° . The gas target consisted of a windowless differentially pumped cell of 8-mm length operated with CH_4 , N_2 , Ne, Ar, and Kr gas at pressures from 1 to 1000 mTorr. Electrons emerging from the interaction region in the forward direction within $\pm 4^\circ$ were analyzed with a standard magnetic spectrograph focusing in two planes, and detected by means of a Channeltron. Beam normalization was achieved with a Faraday cup. Typical analyzing-field strengths in the cusp region were ≈ 20 G. A more detailed description of the apparatus is given in Ref. 12.

Momentum ($\Delta p/p$) and angular resolution Θ_0 of the spectrograph were defined by pairs of apertures which could be varied from 0.2% to $\approx 2\%$ and 0.2° to 1.2° , respectively. These values were calculated from geometry using ray-tracing techniques and experimentally verified by resolving a series of known *KLL* Auger lines from O^{5+} beams.¹³ We note that our Θ_0 values, which are smaller than those used in most other experiments, are necessary for an easy observation of the newly reported behavior of cusp shapes. In order to obtain adequate alignment the spectrometer could be moved parallel and perpendicular to the beam direction and rotated around the target center.

The magnetic field of the Earth and stray fields were reduced to less than 0.05 G at Mumetal shielding. Background electrons could be reduced by applying -300 -V bias to the front electrode of the Channeltron and by careful design of all apertures. A transverse field of some 100 V/cm was applied in front of the gas cell in order to deflect all electrons produced at the beam collimation apertures. Vacuum in the chamber was 10^{-6} Torr and did not exceed 10^{-5} Torr when the highest target pressures were used. As a result, the signal without target gas was less than 1% compared with that for typical gas pressures (100 mT cm) and no background subtraction was necessary. The signal was found to vary linearly with pressure, indicating that single-collision condi-

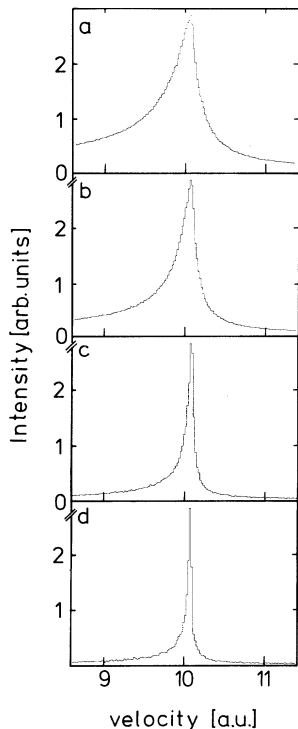


FIG. 1. Cusp-electron spectra of 40-MeV oxygen ions (8+) incident on Ne gas for different spectrometer semiangles Θ_0 : (a) 1.2°, (b) 0.8°, (c) 0.4°, and (d) 0.2°.

tions were fulfilled.

Results for 40-MeV O^{8+} incident on neon are displayed in Fig. 1 for various angular resolutions. For the largest value of $\Theta_0 = 1.2^\circ$ the observed cusp shape agrees well with previous results obtained for $\Theta_0 = 1.8^\circ$ (Ref. 9). When smaller apertures are used, however, we observe two unexpected effects. (1) The ratio of intensities I_R and I_L in the right and left wings of ECC and ELC cusps taken at $\approx 1.1v_p$ and at $\approx 0.9v_p$, respectively, depends strongly on Θ_0 (Fig. 2). (2) The shape and (for ECC) asymmetry of the cusp vary markedly with Θ_0 (Fig. 3).

As regards (1), a ratio with at most a very weak dependence on Θ_0 is expected for both the cusp wings and other contributions to the spectrum such as the relatively small amount of secondary electrons. Furthermore, intensities should scale in proportion to Θ_0^2 (except for the cusp center), but Fig. 4 reveals that a significant Θ_0^n ($n > 2$) contribution is present. Incidentally, the ratio I_L/I_R is larger than 1 for ECC, but smaller than unity for ELC (Fig. 2). Although the total (FWHM) width $\Gamma = \Gamma_L + \Gamma_R$ of ECC cusps is found to be close to the theoretical value $3v_p\Theta_0/2$, the asymmetry Γ_L/Γ_R shows a strong and unexpected increase with Θ_0 (Fig. 3), which levels off for $\Theta_0 > 1^\circ$. It should be stressed that the intensity ratios shown in Figs. 2-4 are quite accurate, because almost all geometrical factors such as solid angle

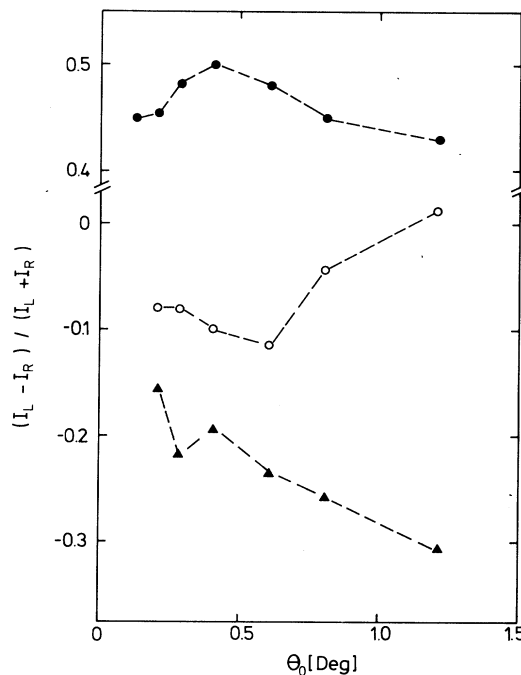


FIG. 2. Ratio $R = (I_L - I_R)/(I_L + I_R)$ of intensities, taken at $\approx 1.1v_p$ in the right (I_R) and at $\approx 0.9v_p$ in the left (I_L) wing of ECC and ELC cusps, as a function of spectrometer semiangle Θ_0 for 40-MeV O^{8+} (\bullet) and O^{5+} (\circ), and 110-MeV Br^{10+} (\blacktriangle) on neon. The dashed lines are drawn to guide the eye.

and momentum resolution drop out.

Before we discuss these findings, we would like to stress that no known artifacts can be responsible for the observed new effects. There is neither a spurious background nor evidence for a sufficiently large contribution of unresolved Auger lines. With the given momentum resolution we can resolve prominent Auger transitions,

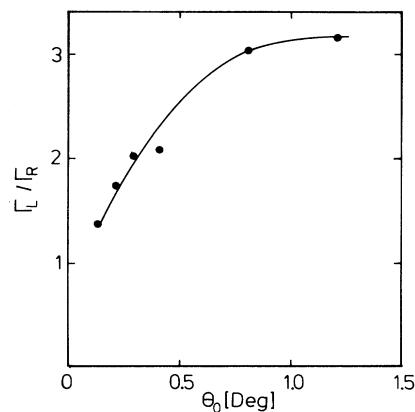


FIG. 3. Cusp-shape asymmetry Γ_L/Γ_R of 40-MeV oxygen (8+) incident on neon, as a function of spectrometer semiangle Θ_0 . The solid line is drawn to guide the eye.

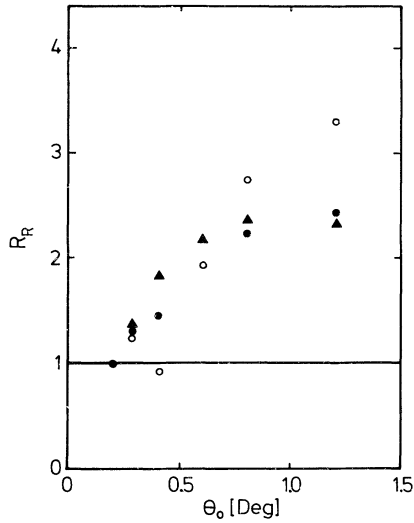


FIG. 4. Intensity ratios $R_R = I_R/\Theta_0^2$ in the right cusp wing, normalized to the value obtained for the smallest spectrometer resolution ($\Theta_0 = 0.2^\circ$), as a function of Θ_0 for 40-MeV O^{8+} (○) and O^{5+} (●), and 110-MeV Br^{10+} (▲) on neon.

but especially for incident O^{8+} and small values of Θ_0 there is no appreciable chance for such (unresolved) transitions. Likewise, for several reasons Rydberg electrons ionized in the deflector field cannot be significant in our spectra: (a) Since the magnetic field does not rise too sharply at the entrance into the magnet, Rydberg electrons become field ionized beneath the trajectory of continuum electrons and cannot reach the detector, especially when Θ_0 is very small. (b) The analyzing field ionizes states not below principal quantum number $n \approx 160$; i.e., the state population is extremely small. In addition, it may be noted that Rydberg states are produced particularly abundantly in foil targets, but our copious data obtained with carbon boils do not show the peculiar effects (1) and (2) observed for gas targets.

At first we tried to analyze our data by means of a frequently used procedure, in which the cross section is represented by a few terms of Legendre polynomials^{7,8,10,11}:

$$\frac{d^2\sigma}{dE d\Omega} \approx \sum_n v^n \sum_l B_{nl} P_l(\cos\Theta) \quad (n \leq 2, l \leq 2), \quad (1)$$

where v is the electron velocity and Θ is the emission angle in the projectile frame. It turns out, however, that application of Eq. (1) to our cusps one at a time (Fig. 1) yields parameters B_{nl} which depend markedly on Θ_0 . Consequently, a simultaneous fit of all cusps (which differ only in Θ_0) does not work satisfactorily. The reason can be traced to the peculiar Θ dependence of the double-differential cross section $d^2\sigma/dE d\Omega$ in the projectile frame. In particular, near $\Theta = 0$ and π we find a slope which is different from zero, expressing a nonanalytic Θ dependence. A nonanalytic function, however, cannot be represented by a truncated expansion Eq. (1).

In principle, inclusion of a large number of terms in Eq. (1) could remedy this problem to some extent, but a practical fit then becomes prohibitive and other procedures must be searched for.

In previous work,⁵ it has been shown that the well-known second Born approximation^{2,4} allows one to describe the asymmetry of ECC cusp shapes:

$$\frac{d^2\sigma}{dE d\Omega} = \frac{v}{2\pi^2 v_P^2} \int_0^{2\pi} d\varphi \int_{k_{\min}}^{\infty} k dk |T_1 + T_2|^2 \quad (2)$$

(in atomic units), where $k_{\min} = [(v_P + v)^2/2 + E_B]/v_P$ is the minimum momentum transfer, and T_1 and T_2 are the scattering amplitudes of the first and the second Born terms. The previously employed high-energy approximation,⁵ however, does not give the presently observed changes of cusp asymmetry as a function of Θ_0 .

In an attempt to describe the newly observed effects, we find that it is necessary and feasible to drop three approximations which have been made in previous calculations⁵: In a refined treatment we take into account (a) the full Coulomb wave without any approximation, (b) the initial binding energy E_B of the captured target electron, and (c) the exact Green's function without linearization. A full presentation of the calculation is beyond the scope of this Letter and we restrict the discussion to the following essential results. In contrast to the asymptotic formulation, inclusion of points (a)–(c) leads to probabilities $|T_1|^2$, $|T_2|^2$, and $|T_1 + T_2|^2$ which are symmetric for small values of final electron momentum k_f , but asymmetric for larger k_f , whereby the degree of asymmetry depends on the collision parameters. Since increasing values of Θ_0 imply experimental observation of larger k_f values, it becomes directly understandable that the associated degree of cusp asymmetry also becomes larger. A typical example of the cross section $d^2\sigma/dE d\Omega$ is displayed in Fig. 5 for oxygen ($8+$) on neon. In view of our theoretical findings it becomes fair to state that, for differing collision parameters, the newly observed Θ_0 dependence is obtained not only because of interference of the amplitudes from the first and second Born approximation but also from a properly calculated first Born amplitude alone.

Incidentally, our model also provides a simple estimate for one of the conditions necessary to observe the new effect in a pronounced manner, namely, $E_B \approx v_P^2/2$ (which is the case in our collision systems). When we inspect previous data for which this condition is also met, anomalies show up in the cusp widths for p on He (Ref. 8, Fig. 8) and O^{8+} on Ne (Ref. 9, Fig. 10), compatible with our present observations.

This theoretical concept also provides an explanation for the ELC case. In ECC we deal with a second scattering event between electron and target atom, so that it becomes reasonable (except for $v_P^2/2 \gg E_B$) to improve the description of ELC by taking into account a second scattering between electron and target ion. A tentative calculation including the target field to higher

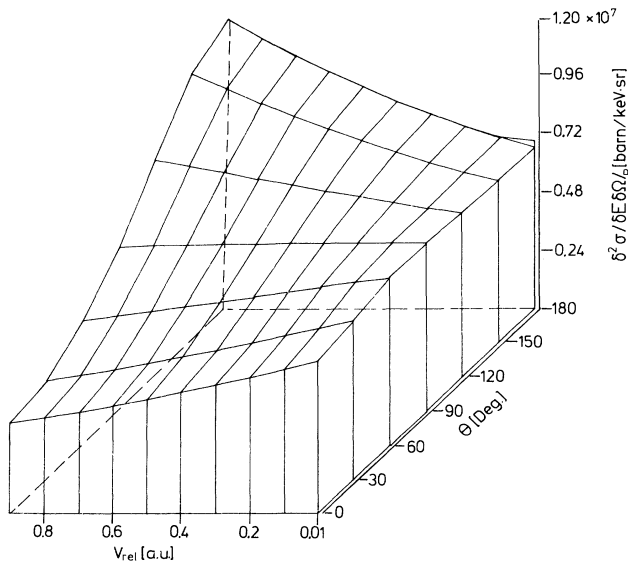


FIG. 5. Double-differential cross section for electron capture to the continuum (ECC) in the projectile frame, as a function of relative electron velocity and emission angle for 40-MeV oxygen ($8+$) on neon.

orders has already been performed¹⁴; one remarkable result is that the ratio I_L/I_R turns out to be smaller than unity (while it is larger than 1 for the ECC case), in qualitative agreement with present observations (Fig. 2). More detailed calculations utilizing the second-order Born approximation for ELC and ECC, along with the presentation of more data, are under way and will be presented separately.¹⁵

In conclusion, we have shown that for many collision systems ECC and ELC cusps can be interpreted better when different experimental angular resolutions Θ_0 are employed and when adequate higher-order theories are utilized such as the second Born approximation. The effect reported here is mainly due to the peculiar behavior of the double-differential production cross section, which must be viewed as one of the characteristic features of both ECC and ELC collision processes, especially when the initial electron binding E_B cannot be

neglected.

We thank D. Jakubassa-Amundsen and M. Kleber for stimulating discussions of many aspects which are important for the development of theoretical calculations. This work was partially supported by Bundesministerium für Forschung und Technologie, Bonn, under Contract No. 6ML177I.

¹G. B. Crooks and M. E. Rudd, Phys. Rev. Lett. **25**, 1599 (1970); K. F. Harrison and M. W. Lucas, Phys. Lett. **33A**, 142 (1970).

²K. Dettmann, K. G. Harrison, and M. W. Lucas, J. Phys. B **7**, 269 (1974).

³F. Drepper and J. S. Briggs, J. Phys. B **9**, 2063 (1976).

⁴R. Shakeshaft, Phys. Rev. A **17**, 1011 (1978).

⁵R. Shakeshaft and L. Spruch, Phys. Rev. Lett. **41**, 1037 (1978).

⁶J. S. Briggs and M. H. Day, J. Phys. B **13**, 4797 (1980).

⁷J. Macek, J. E. Potter, M. M. Duncan, M. G. Menendez, M. W. Lucas, and W. Steckelmacher, Phys. Rev. Lett. **46**, 1571 (1981).

⁸W. Meckbach, I. B. Nemirovsky, and C. R. Garibotti, Phys. Rev. A **24**, 1793 (1981).

⁹M. Breinig, S. B. Elston, S. Hultdt, L. Liljeby, C. R. Vane, S. D. Berry, G. A. Glas, M. Schauer, I. A. Sellin, G. D. Alton, S. Datz, S. Overbury, R. Laubert, and M. Suter, Phys. Rev. A **25**, 3015 (1982).

¹⁰H. Knudsen, L. H. Andersen, and K. E. Jensen, J. Phys. B **19**, 3341 (1986).

¹¹Y. C. Yu and G. Lapicki, Phys. Rev. A **36**, 4710 (1987).

¹²R. Schramm, W. Oswald, H.-D. Betz, E. Szmola, and R. Schuch, in *High-Energy Ion-Atom Collisions*, edited by D. Berényi and G. Hock, Lecture Notes in Physics Vol. 294 (Springer-Verlag, Berlin, 1988), p. 277.

¹³N. Stolterfoht, in *Structure and Collisions of Ions and Atoms*, edited by I. A. Sellin, Topics in Current Physics Vol. 5 (Springer-Verlag, Berlin, 1978), p. 155–199 (see Fig. 5.4 for O^{5+} on Ne).

¹⁴D. H. Jakubassa-Amundsen, in *Forward Electron Ejection in Ion Collisions*, edited by K. O. Groeneveld, W. Meckbach, and I. A. Sellin, Lecture Notes in Physics Vol. 213 (Springer-Verlag, Berlin, 1984), p. 17 (see Fig. 8).

¹⁵W. Oswald, R. Schramm, H.-D. Betz, and D. H. Jakubassa-Amundsen (to be published).